STScI | SPACE TELESCOPE SCIENCE INSTITUTE

Instrument Science Report COS 2019-06(v1)

Focusing the New COS/FUV Cenwave G160M/1533

Bethan L. James[1], Andrew J. Fox[1], and Elaine M. Frazer[1]

[1] Space Telescope Science Institute, Baltimore, MD

24 June 2019

ABSTRACT

In Cycle 26 two new central wavelengths (cenwaves) were commissioned for Lifetime Position 4 (LP4) of the COS FUV detector: G160M/1533 and G140L/800. This ISR describes the first stage of this commissioning program for G160M/1533, providing an optimized focus value for the cenwave. In 2018 March a focus sweep program was performed using observations of Feige 48 at a range of focus settings relative to the closest current observational setup, G160M/1577. An auto-correlation technique was used to find the minimal line widths of stellar absorption lines versus focus value and therefore find the optimal focus setting. This yielded a (breathing corrected) focus value of +85 steps relative to the focus value of G160M/1577; i.e., an absolute focus value of $f = -731$ for G130M/1533. This final derived focus offset was added to the flight software tables for use in all subsequent G160M/1533 observations.

Contents

Operated by the Association of Universities for Research in Astronomy, Inc., for the National Aeronautics and Space Administration.

1. Introduction

For Cycle 26 two new central wavelength (cenwave) settings were introduced for the COS FUV detector, G140L/800 and G160M/1533. The 1533 cenwave extends coverage at the short-wavelength end of G160M by 44 Å to overlap with the longest wavelengths covered by cenwave G130M/1222. This allows a broad range of FUV wavelengths to be covered by just two medium-resolution settings (1222 and 1533) without placing Lyα on the detector, avoiding a key contributor to gain sag. Furthermore, it allows the full FUV bandpass to be observed at high S/N, since all four FP-POS positions can be used with both 1222 and 1533. This mitigates fixed-pattern noise and allows a higher S/N in the co-added spectrum. This report forms one of a number of ISRs on the calibration of the new 1533 cenwave. Here we describe how we determined the optimal focus for the 1533 cenwave. This ISR is a partner to the ISRs on the creation of the lamp template (LAMPTAB; James et al. 2019), the spectral extraction algorithm (XTRACTAB, TWOZXTAB, PROFTAB, TRACETAB; Frazer et al. 2019), the wavelength calibration (DISPTAB, Fox et al. 2019a), and the flux calibration (FLUXTAB, Fox et al. 2019b). Together these reference files were delivered to the CRDS database on 2018 November 20, updated for both 1533 and 800, for use with Cycle 26 observations.

When commissioning a new cenwave we need to derive its optimal focus value. We can predict the focus value by extrapolating the known focus-wavelength relation for that grating to the wavelength of the new cenwave (Ake et al. 2019). The optimal focus values are then determined by performing a "focus sweep" around this predicted focus, where a stellar spectrum is obtained at a number of focus positions, and the spectral line width is analysed at each position to determine which position yields the sharpest stellar absorption lines. The focus value which represents the "best focus" for this cenwave is then specified as an absolute focus value encoded in the flight software, for use in subsequent observations at Lifetime Position 4 (LP4).

It should be noted that in previous focus sweep analyses, the final focus value is compared to expectations from ray-trace models (e.g., Fox et al. 2017, Sonnentrucker et al. 2017). However, such models were not generated for G160M/1533, therefore prohibiting such a comparison.

2. Observations and Data Reduction

The G160M/1533 focus-sweep involved COS/FUV observations of the star Feige 48 with the G160M/1577 setting for four external orbits in a single visit. Feige 48 is a subdwarf B star with a low projected rotational velocity and many narrow photospheric

Table 1. Exposures and Focus Offsets for G160M/1533 Focus Sweep (PID 15452)

Filename	Start Time	Commanded Focus Offset	Breathing-corrected Focus Offset
lds201eaq	03/15/2018 03:46:45	−1000	−919
lds201efq	03/15/2018 04:39:48	−800	−832
lds201ehq	03/15/2018 04:52:04	−600	−578
lds201ejq	03/15/2018 05:04:20	−400	−352
lds201esq	03/15/2018 06:15:06	−300	−337
lds201euq	03/15/2018 06:27:20	−200	−185
lds201ewq	03/15/2018 06:39:34	−100	−47
lds201eyq	03/15/2018 07:50:23	0	−18
lds201f0q	03/15/2018 08:02:37	100	119
lds201f2q	03/15/2018 08:14:51	200	250
lds201f4q	03/15/2018 09:25:41	300	287
lds201f6q	03/15/2018 09:37:55	400	424
lds201f8q	03/15/2018 09:50:11	600	659
lds201faq	03/15/2018 10:02:27	800	878
lds201fcq	03/15/2018 11:00:58	1000	970

absorption lines (widths < 5 km s^{-1}) in the UV, rendering it an ideal target for this focus sweep, which relies on a line-width analysis.

The data were obtained in 2018 March (as detailed in Table 1). The sweep was performed by scanning at 200 focus-step increments from -1000 to $+1000$ from the estimated focus at 1533 (extrapolated from the current G160M cenwave settings to be $f = -731$), a strategy designed to determine the best focus position to within 1% accuracy. This strategy is based on previous focus sweep programs (PIDs 14874 and 12505), which obtained sweeps for G160M/1600 at LP4 and the G130M/1222 cenwave, respectively (Fox et al. 2017, Sonnentrucker et al. 2017). In addition, finer focus steps of 100 in size were used between -400 and $+400$ in order to better sample the focus curve near the central minimum.

Designing the Phase II observations required special commanding since the 1533 cenwave was not implemented in the APT proposal planing software at the time of execution. After an ACQ/IMAGE target acquisition with MIRRORA/BOA, an initialization exposure was used to configure G160M/1577, as this is the closest instrument mode to G160M/1533. The OSM1 mechanism was then aligned (using the ALIGN/OSM command) to -1000 steps from the G160M/1533 predicted focus value ($f = -731$, as determined from extrapolation from all G160M focus values as a function of cenwave). It should be noted that the focus value supplied for the

ALIGN/OSM command was relative to the absolute focus value of G160M/1577 ($f = -108$), i.e. FOCUS $= -731 - 1000 - (-108) = -1623$. An additional keyword was set, OSMROT1 $= 15$, which is the OSM rotation position offset between c1533 and c1577 according to ray-trace optical models (S. Penton, private communication) to prevent the OSM from defaulting to OSMROT1 $= 0$ when subsequent focus values were commanded. Between each focus change, Feige 48 spectra were obtained with a poisson S/N ~ 30 at 1550 Å, for FP-POS $= 3$ using exposures times of 545 s. At the end of the focus sweep, the focus value offset and OSMROT1 parameters were reset to their values for G160M/1577.

We used special commanding to switch off calibration and disassociate the 1533 exposures, since the back-end software was (at the time of execution) not ready for processing 1533 files. The program was executed before mid-March 2018 to ensure that a focus value for G160M/1533 would be delivered to the CRDS database by the end of that month.

The data were manually reduced using CalCOS. During the reduction, DOPPCORR was performed to correct for HST orbital motion (which can cause $\sim$15 km s^{-1} of line broadening. This required us to use a DISPTAB that had been manipulated by replacing the 1577 dispersion solution entries by placeholder values for 1533. These placeholder 1533 DISPTAB entries (zeropoint and dispersion) were predicted from the other G160M cenwave values. WAVECORR was set to OMIT during the reduction process since the LAMPTAB for 1533 had not been created at this point. Flatfielding was performed using the gridwire-only flat created during the LP4 lifetime move (Ely et al. 2011). The reduction process created `corrtag` FITS files (in XDOPP/YCORR space) which were corrected for thermal, geometric, and walk effects. Two-dimensional spectral images were created from the `corrtag` events, and subsequent 1D spectra were extracted. Since the focus sweep analysis occurs in wavelength space, the pixels within the extracted spectra were converted into wavelengths using the 1533 dispersion solution placeholder values used in the DISPTAB. The focus analysis was performed on the final 1D spectra.

The minimum of the focus curve can only be found after correcting the focus values for thermal breathing of the telescope, as this can cause an offset between the actual and commanded focus position. The breathing correction is derived from a model, based on temperatures measured via sensors on the telescope. The *HST* focus model tool[1] computes the focus offset with respect to the nominal value at the time of observations using WFC3/UVIS1 data. As with all previous focus sweeps performed for COS, the focus offsets measured for WFC3 are assumed to be identical to those experienced by COS. This tool is used to determine the breathing-corrected focus offset at the start of each exposure in the program (Figure 1). Corrected offset values are defined as the commanded focus offset minus the breathing correction (in microns). In order to translate the focus offsets experienced by WFC3 into units of COS/OSM1 focus steps, the offsets are multiplied by a factor of 19.2 (see Oliveira et al. 2013).

[1] http://focustool.stsci.edu/cgi-bin/control.py

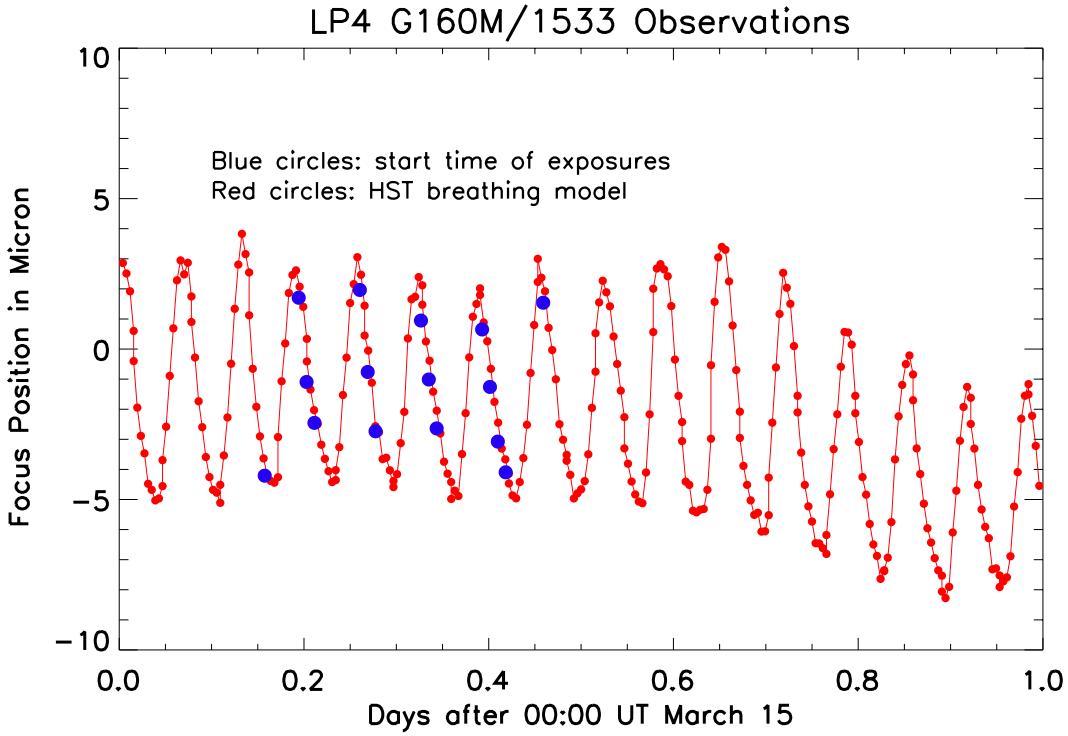

Figure 1. The WFC3/UVIS1 focus position as a function of time (red points) and corresponding breathing model (red line), throughout the period of time when PID 15452 (G160M/1533 Focus Sweep) was executed. The cycle has a period of one *HST* orbit and illustrates the thermal breathing of the telescope. Overlaid in blue points are the times at which each exposure in the focus sweep began (Table 1). The focus sweep analysis is performed on breathing-corrected focus offsets; i.e., commanded focus values minus the breathing correction.

Table 2. Wavelength Ranges for Auto-Correlation and Derived Focus Offsets[1]

Setting	$\delta\lambda_1$ (Å)	δf_1	$\delta\lambda_2$ (Å)	δf_2
G160M/1533/FUVA	1540–1665	-17	1673–1702	$+15$
G160M/1533/FUVB	1358–1385	$+430$	1410–1500	$+134$

[1]Each spectral window was selected to be free from both strong interstellar lines and geocoronal emission.

3. Data Analysis

In accordance with previous focus sweeps, the best-fit focus value for G160M/1533 is determined using an auto-correlation method. In order to perform this auto-correlation, regions of spectra that contain narrow absorption lines are chosen and cross-correlated with themselves. Regions of spectra containing ISM absorption lines and airglow emission (i.e., from Lyα or O I λ1302) are avoided. The selected wavelength windows are given in Table 2.

Determining the best focus value requires a two-step process. Firstly, the widths of the absorption lines within each spectral window or wavelength range are derived using an auto-correlation function (ACF). The ACF is essentially a statistical measure of the width, thus representing the spectral resolution and focus, such that a narrow ACF represents narrow absorption lines and a well focused spectrograph. To determine the width of each ACF, the ACF is calculated for each position in the focus sweep, normalized with a peak of one, and fitted with a Gaussian.

Secondly, the ACF width for each focus value is then plotted as a function of corrected focus offset. These focus curves are shown in Figure 2, along with the best-fit focus offset for each spectral window. This best-fit value is obtained from the minimum of each focus curve found by fitting a cubic function to the curve. As with previous focus sweeps, a cubic function was found to give a good representation of the G160M grating focus curve. Given that we calculate the ACF across an entire spectral window, the best-fit focus value derived for each window essentially represents the optimal resolution for the average wavelength within the wavelength range of that window. The full-width at half-maximum (FWHM) of the ACF is also calculated for each spectral window, in order to verify that the focus curves show similar minima for both the FWHM and Gaussian widths. However, we adopt the Gaussian width in our final analysis following the strategy used in the LP3 focus sweep (Fox et al. 2015).

Upon inspection of the focus curves for individual spectral regions, it was found that the minima of the focus curves for FUVA 1673–1702 Å and FUVB 1358–1385 Å

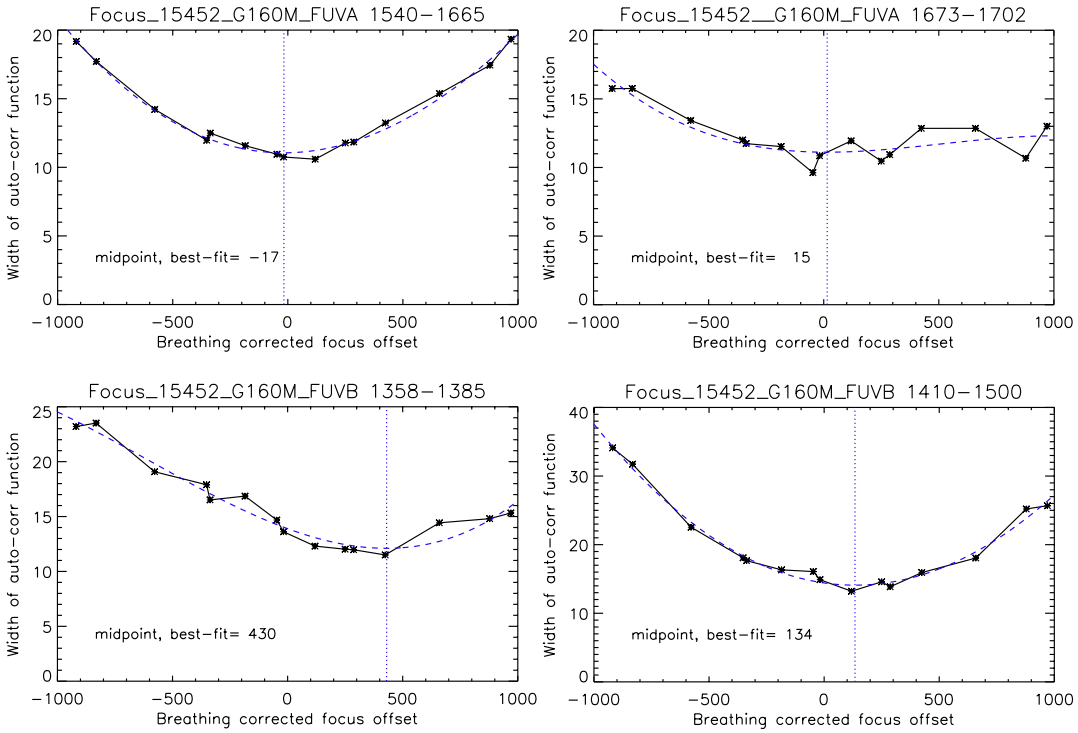

Figure 2. Focus curves derived for each spectral window listed in Table 2. The width of the ACF is plotted against the breathing-corrected focus offset relative to LP4. The derived best-fit focus offset for each curve, printed in each panel, is defined as the minimum of the cubic fit shown with the blue dashed curve.

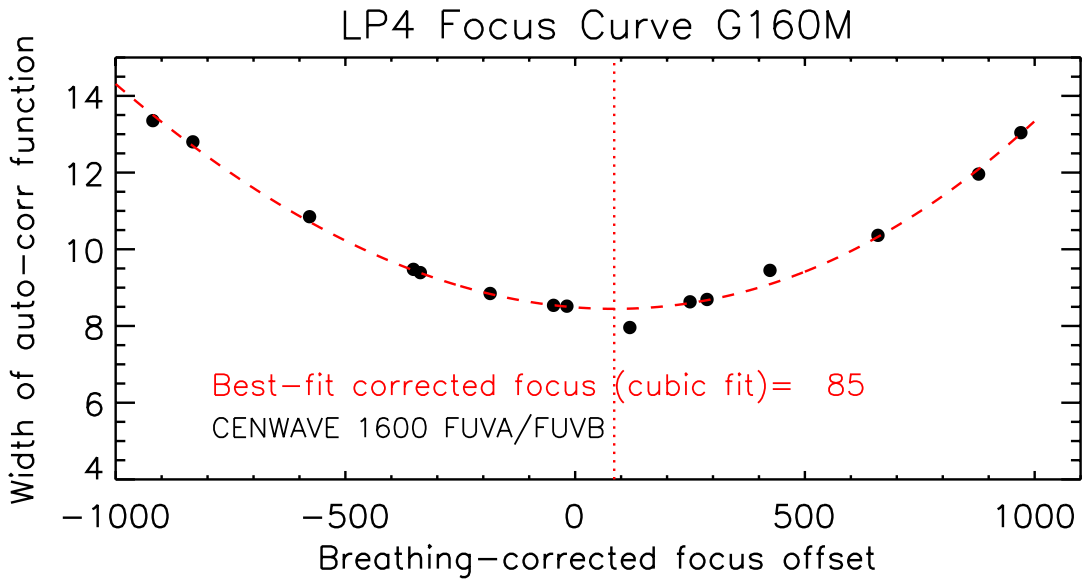

Figure 3. The final focus curve for the G160M/1533 setting, derived from spectral windows FUVA 1540–1665 Å and FUVB 1410–1500 Å. The width of the ACF is plotted against the breathing-corrected focus offset relative to LP4. Our adopted best-fit focus offset (+85) is the minimum of the cubic fit shown with the red dashed curve.

were not well defined in comparison to that of FUVA 1540–1665 Å and FUVB 1410–1500 Å. As such they were not included when deriving the final average best-fit focus value. The final best-fit focus curve derived from FUVA 1540–1665 Å and FUVB 1410–1500 Å is shown in Figure 3, annotated with the best-fit focus corrected focus value of +85 relative to the expected focus of −731, giving a final absolute best-focus of −646. It should be noted that the difference between the final best-fit focus (−646) and the extrapolated value (−731) was not unsurprising, since 1533 is a large number of focus motor steps away from 1577, and it is unclear whether a linear extrapolation is valid over such a large range.

In order to visually inspect and validate our final best-fit focus value, regions of spectra that include strong interstellar absorption or photospheric lines were chosen from our focus sweep data and plotted for each focus position. If our ACF technique is successful, the spectrum at the focus closest to the best-fit focus value should display the narrowest lines. Figure 4 shows the data between 1380 and 1415 Å, covering the Si IV $\lambda\lambda$1393, 1402 doublet. The relative best-fit focus found from the ACF technique was found to be at +85 and as such, the spectra should show the narrowest lines at the corrected (relative) focus of +119. However, given the shallow nature of the focus curve between $f = -300$ and +300, this widening is only observed beyond these focus offset values.

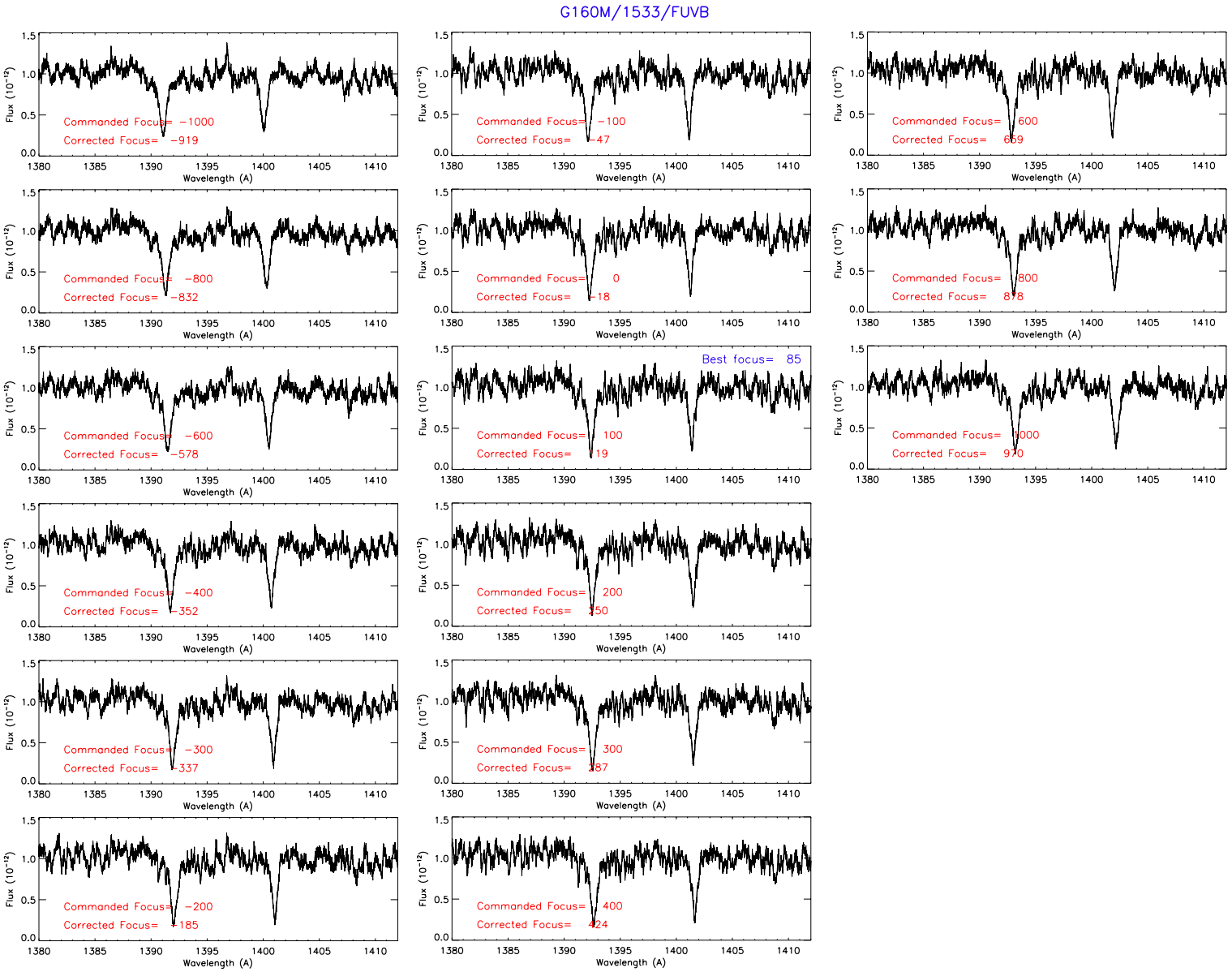

Figure 4. The Si IV $\lambda\lambda$1393, 1402 interstellar and wind absorption line doublet observed in the Feige 48 spectra. Spectra from each of the 15 focus steps used in the sweep are shown as individual panels. Printed in each panel are the commanded and breathing-corrected focus offset values. Fluxes are in units of erg s^{-1} cm^{-2} Å^{-1}. The best-fit focus for G160M/1533 determined from our auto-correlation analysis (+85) is annotated on the panel with the closest-matching corrected focus (+119). This panel can be seen to show sharply focused absorption lines, while the panels showing focus values above and below this value are seen to progressively widen. However, since the focus curve is relatively shallow between ±300 focus offset values, the widening with focus value is only seen in panels with focus offsets larger than these values.

4. Results and Conclusions

The focus value for G160M/1533, a new cenwave commissioned for Cycle 26 and beyond, was found to be at COS/OSM1 focus step $f = -646$. This value is $+85$ steps relative to the predicted focus value of $f = -731$, as determined from extrapolation from all G160M focus values as a function of cenwave. This value was supplied to the flight software as a focus offset relative to the current value encoded in the flight software table `Pcmech OSMtbl`, which is found in the flight software file `pcmech.c`, for use in all subsequent G160M/1533 observations.

Acknowledgments

The authors acknowledge the use of the *HST* Focus Model tool provided by Colin Cox.

Change History for COS ISR 2019-06

Version 1: 24 June 2019 – Original Document

References

Ake, T., Plesha, R., De Rosa, G., et al. 2019, COS ISR 2018-23, "Improvements to the COS FUV G130M and G160M Wavelength Solutions at Lifetime Position 2"

Ely, J., Massa, D., Ake, T., et al. 2011, COS ISR 2011-03, "COS FUV Gridwire Flat Field Template"

Fox, A. J., James, B. L., Frazer, E. M., & Fischer, W. J. 2019b, COS ISR 2019-09, "The Flux Calibration of the New COS/FUV Cenwave G160M/1533"

Fox, A. J., James, B. L., Frazer, E. M., Plesha, R., & Ake, T. 2019a, COS ISR 2019-10, "The Dispersion Solution for the New COS/FUV Cenwave G160M/1533"

Fox, A., Oliveira, C., Penton, S., et al. 2015, COS ISR 2015-01, "The COS/FUV Focus Sweep Program at Lifetime Position 3 (LENA2/13635)"

Fox, A., Penton, S., & Taylor, J. 2017, COS ISR 2017-17, "Focusing the COS/FUV G160M and G140L Gratings at Lifetime Position 4"

Frazer, E. M., Fox, A. J., James, B. L., Roman-Duval, J., & Sankrit, R. 2019, COS ISR 2019-08, "Spectral Extraction of the New COS/FUV G160M/1533 Mode: Extraction, Trace, and Profile Reference Files"

James, B., et al. 2019, COS ISR 2019-07, "The Lamp Template for the New COS/FUV Cenwave G160M/1533"

Oliveira, C., Bostroem, A., & Osterman, S. 2013, COS ISR 2013-01, "Second COS FUV Lifetime Position Results from the Focus Sweep Enabling Program, FENA3 (12796)"

Sonnentrucker, P., Fox, A., Penton, S., et al. 2017, COS ISR 2017-16, "FUV Focus Sweep Exploratory Program for COS at LP4"